Rice husk derived carbon–silica composites as anodes for lithium ion batteries†

Liping Wang,*[a] Jing Xue,[a] Bin Gao,[a] Peng Gao,[b] Chengxu Mou[a] and Jingze Li[a]

Carbon–silica composites were obtained *via* simply heating rice husk at 900 °C under a N_2 atmosphere. This composite exhibits a high capacity and superior cycling performance as an anode for lithium ion batteries.

Energy consumption is concomitantly growing with economic growth and the world's population expansion. Due to limited fossil sources, developments of clean, alternative, and sustainable energy technologies are imperative.[1] In parallel, the intermittent renewable energies (*e.g.* wind, solar, hydro/geothermal) need the implementation of highly efficient energy storage devices. As of today, lithium ion batteries (LIBs) are the contenders for these power source systems, which have been widely used in portable electronics and present a promising future in electric vehicles and hybrid electric vehicles.[2]

Electrode materials with sustainable and low cost features are the primary choices for the next-generation high performance LIBs. In this respect, natural-born biomass related materials with zero CO_2 emissions are the best candidates. According to the-state-of-the-art, carbon derived from biomass (*e.g.* banana fibers, charcoal, peanut shell) has been investigated for high capacities and good capacity retentions anodes for LIBs.[3–7] Among them, rice husk with a global production of 600 million tons per year is one of the most common agriculture wastes. The main components of rice husk are hydrocarbon compounds (cellulose, lignin, and hemicelluloses) and silica.[8] In our pervious study,[9] we used hydrothermal carbonization method to fabricate carbon fibers from rice husk with removal of silica as anodes for lithium ion batteries, which showed superior capacity retentions and rate capabilities. Recently, Liu

et al. took the advantages of SiO_2 in rice husk to produce Si by Mg reduction.[10,11] The as-obtained Si with nanosize and porous characteristic delivered high reversible capacity (2790 mA h g^{-1}) and long cycling life with retention of 86% after 300 cycles as anodes for LIBs.[10]

The study of C/SiO_2 composites from biomass as electrode materials has not been performed yet since the silica is generally considered to be electrochemically inactive. In fact, it has been reported that nanosize or porous SiO_2 towards electrochemical activity.[12–15] Sun *et al.* firstly reported that SiO_2 thin film obtained by radio frequency sputtering demonstrated reversible capacity of more than 400 mA h g^{-1} in a SiO_2/Li half cell.[13] As for rice husk, SiO_2 naturally exists in nanosize form and accumulates around cellulose components.[10,16] Watari *et al.* fabricated porous C/SiO_2 composites pellets with a surface area of 450 m^2 g^{-1} and pore size distribution of about 2 nm through a simply calcination of rice husk.[17] Inspired by these concepts, we directly combust the rice husk under inert atmosphere to obtain porous C/SiO_2 composites and their electrochemical performance as anodes for lithium ion batteries is evaluated. To our best knowledge, it is the first time to report C/SiO_2 composites from biomass as anodes for lithium ion batteries.

The elemental analysis of RH and RH-900 is provided in Table 1. As is known to us, the major components of lignocelllulose biomass materials are cellulose, lignin, hemicelluloses, and silica. In our cases, the carbon takes up 33.56 wt% of the pristine RH. Except C, N, S, and H elements, the other elements those could not be detected are mainly attributed to oxygen and silicon. From our TG analysis,[9] 29 wt% of SiO_2 was detected *via* combustion of the pristine RH in O_2

[a]State Key Laboratory of Electronic Thin Films and Integrated Devices, University of Electronic Science and Technology of China, Chengdu 610054, China. E-mail: lipingwang@uestc.edu.cn

[b]Institute of Engineering Innovation, The University of Tokyo, 2-11-16 Yayoi, Bunkyo, Tokyo 113-8656, Japan

Table 1 Elemental analysis of RH and RH-900

Sample	N%	C%	H%	S%	Others
RH	0.40	33.56	4.78	0.98	60.29
RH-900	0.68	41.08	1.06	1.00	57.18

atmosphere. After calcinations at 900 °C in inert atmosphere, the carbon takes up 41.08 wt% in the total weight and others (mainly SiO_2, other constituents of rice husk ash, such as Fe_2O_3, K_2O, Al_2O_3, CaO, MgO, Na_2O, are less than 1%[18]) take up of 57.18 wt%.

Fig. 1 shows the typical TEM characterizations of RH-900. Its SEM images and corresponding EDX images of elemental C and Si are show in Fig. S1.† The surface of the pristine RH from SEM images was smooth in low magnification. Actually, during the heat treatment in inert atmosphere, organic compounds decompose and partially change to H_2O, CO, CO_2, and volatile compounds.[18] It can lead a porous structure, which is seen in the high angle annular dark field STEM (Z-contrast) image of Fig. 1a. Under this condition, heavier SiO_2 has a brighter contrast than carbon. The size of SiO_2 ranges from 10 nm to 50 nm, which is consistent with the study of Jung *et al.*[11] Meanwhile, the carbon and SiO_2 were homogeneously distributed in the RH-900 (Fig. 1b and S1c and d†), which means that the C/ SiO_2 is a natural born composite. This composite (Fig. 1d) shows almost amorphous features with weak diffraction rings corresponding to (002) and (100) planes of pyrolytic carbon,[19] complying with our XRD results (Fig. S2†). Its corresponding Raman spectroscopy and nitrogen sorption isotherms (BET surface area 270 m^2 g^{-1} and pore volume 0.15 cm^3 g^{-1}) are provided in Fig. S3 and S4,† respectively.

The electrochemical properties of a RH-900/Li cell are displayed in Fig. 2. The first three cyclic voltammograms for the as-prepared RH-900 electrode between 0 V and 3.0 V measured at a scan rate of 0.02 mV s^{-1} are shown in Fig. 2a. As for the electrochemical reaction of SiO_2 with Li, several mechanisms were proposed.[12–15] Whereas it is still difficult to draw a
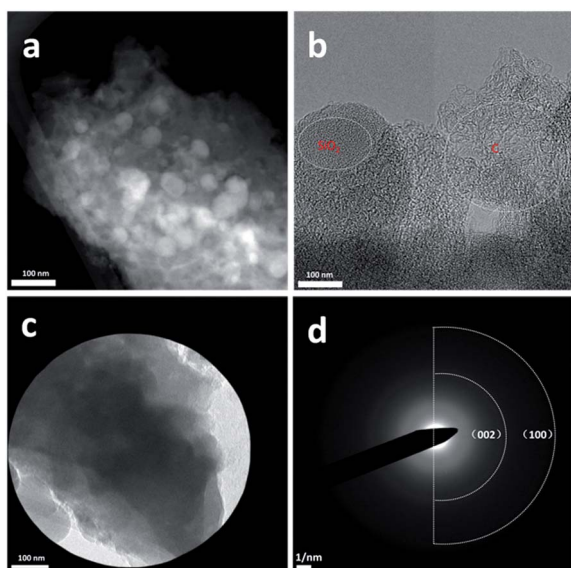

Fig. 1 (a) A Z-contrast (high angle annular dark field) STEM image of RH-900, (b) high magnification TEM image of RH-900 showing amorphous SiO_2 and weak crystalline nature of carbon, (c) bright-field TEM images and (d) corresponding selected area electron diffraction patterns of RH-900.
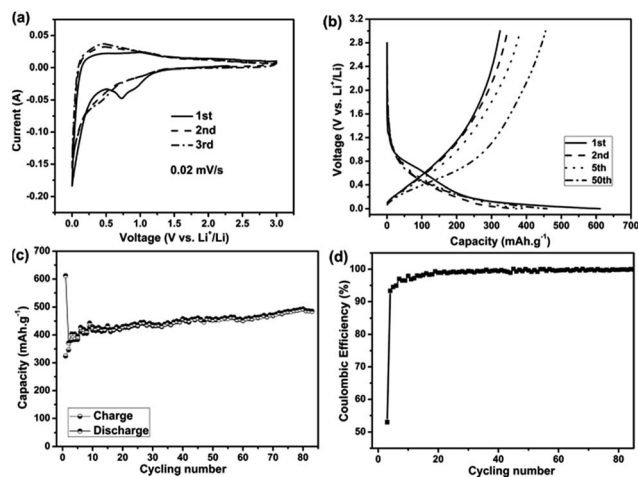

Fig. 2 Electrochemical performance of RH-900 as an anode for LIBs. (a) Cyclic voltammetry of RH-900 at a scan rate of 0.02 mV s^{-1}, (b) charge–discharge profiles of RH-900 at 1st, 2nd, 5th and 50th cycle in the voltage range of 0–3.0 V. (c) Cycling performance of RH-900, (d) Coulombic efficiency of RH-900.

conclusion owing to the difficulty in identifying the almost amorphous crystal structure of the silicates and various valence states of Si in the Li–Si alloys. In our case, the SiO_2 was electrochemically reduced to produce $Li_2Si_2O_5$ or Li_4SiO_4 and Si first (∼0.79 V), then for the formation of Li–Si alloy (below 0.25 V) in the initial discharge process, which is consistent with the results of Guo *et al.*[14] During the charge process, the anodic peaks were not well resolved, which coincides with the typical report of the C and SiO_2 materials.[15,20] It is worthy to note that the anodic and cathodic current intensities increased with the cycles (from the second cycle) indicating that the charge– discharge capacity increases in their following cycles. The corresponding galvanostatic charge–discharge curves are shown in Fig. 2b. These voltage profile signatures are in good agreement with the cyclic voltammograms measurements. It is known that pyrolytical carbon with disordered structure often demonstrates lithium storage capacity of more than the theoretical capacity 372 mA h g^{-1} of graphite. For a comparison, we also tested the electrochemical properties of individual carbon and silica in the mixture (Fig. S5†) under the same current rate of 74 mA g^{-1}. The carbon derived from RH-900 after removal of silica *via* NH_4HF_2 showed an average reversible capacity of about 300 mA h g^{-1}. The silica derived from the RH-900 after calcination at 500 °C under O_2 atmosphere demonstrated an average reversible capacity of 40 mA h g^{-1}. Here, C/SiO_2 (RH-900) demonstrated an initial discharge capacity of 325 mA h g^{-1}. Note that this capacity is obtained by using the active weights of C/SiO_2 (41.08 wt% : 58.92 wt%) composites. If we simply calculate the carbon as an active material and consider the SiO_2 as an inert component, it can be inferred that the discharge capacity is 791 mA h g^{-1}, which is much higher than carbon materials, indicating that silica in our mixture has electrochemical activity. Since the theoretical capacity of SiO_2 are more than 749 mA h g^{-1} based on different mechanisms.[15] It means that

our SiO$_2$ in the RH-900 has comparatively low electrochemical activity. We believe that the SiO$_2$ with size of 10–50 nm is not small enough to achieve full electrochemical capacity. It is interesting to note that the capacity is continuous increase with the increase of cycling number (Fig. 2c). The initial discharge capacity of 325 mA h g^{-1} increased to 485 mA h g^{-1} after 84 cycles, suggesting that an electrochemical activation of C/SiO$_2$ is responsible for the increased capacity. Since our SiO$_2$ has the size distribution from 10–50 nm, we presume that the surface part of SiO$_2$ is electrochemically active. The inner part of SiO$_2$ are inactive but be activated in the later cycles. It is noted that the SiO$_2$ not only contributes to the electrochemical activity but also acts as "*in situ*" hard template framework to keep the structure stable thus to improve its electrochemical capacity retention behavior. The discharge and charge capacity of the first cycle are 611 mA h g^{-1} and 325 mA h g^{-1}, respectively, with a low initial Coulombic efficiency of 53% (Fig. 2d), which is quite low probably due to the related structure of composite C/SiO$_2$ itself as well as the parasitic reaction of electrolyte reduction to the formation of solid electrolyte interphase (SEI). The Coulombic efficiency recovered to ~97% after several cycles, presumably due to the structure activation and incomplete stabilization of SEI. In all, compared with the most successful commercial anode materials of graphite, which is normally obtained at high temperature >2000 °C and has a theoretical capacity of 372 mA h g^{-1},[21] our C/SiO$_2$ composites obtained *via* a *chimie-douce* and sustainable way display higher capacity as well as better capacity retention behavior.

In summary, C/SiO$_2$ composites synthesized *via* one-step fire process of rice husk were applied as anode electrodes for lithium ion batteries for the first time. It showed an initial discharge capacity of 325 mA h g^{-1} and increased to 485 mA h g^{-1} after 84 cycles. The presence of SiO$_2$ with nanosize 10–50 nm in this composite not only has electrochemical activity but also plays a role in stabilizing the structure of the electrode. This low cost, facile, and sustainable strategy brings new perspectives in the utilization of biomass waste as electrodes for energy storage devices.

References

1 H. Chen, M. Armand, G. Demailly, F. Dolhem, P. Poizot and J. M. Tarascon, *ChemSusChem*, 2008, **1**, 348–355.
2 J. B. Goodenough and Y. Kim, *Chem. Mater.*, 2010, **22**, 587–603.
3 G. T. K. Fey, Y. D. Cho, C. L. Chen, Y. Y. Lin, T. P. Kumar and S. H. Chan, *Pure Appl. Chem.*, 2010, **82**, 2157–2165.
4 T. Liu, R. Y. Luo, W. M. Qiao, S. H. Yoon and I. Mochida, *Electrochim. Acta*, 2010, **55**, 1696–1700.
5 F. Zhang, K. X. Wang, G. D. Li and J. S. Chen, *Electrochem. Commun.*, 2009, **11**, 130–133.
6 A. Caballero, L. Hernan and J. Morales, *ChemSusChem*, 2011, **4**, 658–663.
7 A. M. Stephan, T. P. Kumar, R. Ramesh, S. Thomas, S. K. Jeong and K. S. Nahm, *Mater. Sci. Eng., A*, 2006, **430**, 132–137.
8 W. Arayapranee, N. Na-Ranong and G. L. Rempel, *J. Appl. Polym. Sci.*, 2005, **98**, 34–41.
9 L. P. Wang, Z. Schnepp and M. M. Titirici, *J. Mater. Chem. A*, 2013, **1**, 5269–5273.
10 N. A. Liu, K. F. Huo, M. T. McDowell, J. Zhao and Y. Cui, *Sci. Rep.*, 2013, **3**, 1919.
11 D. S. Jung, M. H. Ryou, Y. J. Sung, S. B. Park and J. W. Choi, *Proc. Natl. Acad. Sci. U. S. A.*, 2013, **110**, 12229–12234.
12 W. S. Chang, C. M. Park, J. H. Kim, Y. U. Kim, G. Jeong and H. J. Sohn, *Energy Environ. Sci.*, 2012, **5**, 6895–6899.
13 Q. Sun, B. Zhang and Z. W. Fu, *Appl. Surf. Sci.*, 2008, **254**, 3774–3779.
14 B. K. Guo, J. Shu, Z. X. Wang, H. Yang, L. H. Shi, Y. N. Liu and L. Q. Chen, *Electrochem. Commun.*, 2008, **10**, 1876–1878.
15 N. Yan, F. Wang, H. Zhong, Y. Li, Y. Wang, L. Hu and Q. W. Chen, *Sci. Rep.*, 2013, **3**, 1568.
16 A. I. Hochbaum, R. K. Chen, R. D. Delgado, W. J. Liang, E. C. Garnett, M. Najarian, A. Majumdar and P. D. Yang, *Nature*, 2008, **451**, 163–165.
17 T. Watari, A. Nakata, Y. Kiba, T. Torikai and M. Yada, *J. Eur. Ceram. Soc.*, 2006, **26**, 797–801.
18 S. Kumagai and J. Sasaki, *Bioresour. Technol.*, 2009, **100**, 3308–3315.
19 L. P. Wang, C. Schutz, G. Salazar-Alvarez and M. M. Titirici, *RSC Adv.*, 2014, **4**, 17549–17554.
20 L. Qie, W. M. Chen, Z. H. Wang, Q. G. Shao, X. Li, L. X. Yuan, X. L. Hu, W. X. Zhang and Y. H. Huang, *Adv. Mater.*, 2012, **24**, 2047–2050.
21 J. R. Dahn, T. Zheng, Y. H. Liu and J. S. Xue, *Science*, 1995, **270**, 590–593.